Article ID: 1003－6326(2003)05－1220－06

Characteristics of electrodeposited RE-Ni-W-B-B_4C-MoS_2 composite coating①

MA Ke-yi(马克毅), GUO Zhong-cheng(郭忠诚), ZHU Xiao-yun(朱晓云), XU Rui-dong(徐瑞东)
(Faculty of Materials and Metallurgical Engineering,
Kunming University of Science and Technology, Kunming 650093, China)

Abstract: The high temperature oxidation resistance of RE-Ni-W-B-B_4C-MoS_2 composite coating, the effects of electrodeposition conditions on the morphologies of the coating and the effect of heat treatment temperature on its hardness, abrasion resistance and phase structure were investigated by using scanning electron microscope(SEM), X-ray diffractometer, microhardness tester and abrasion machine. The results show that the oxidation degree of RE-Ni-W-B-B_4C-MoS_2 composite coating is small when the temperature is lower than 700 ℃, but it increases sharply when the temperature is higher than 700 ℃. The hardness of RE-Ni-W-B-B_4C-MoS_2 composite coating increases with increasing heat treatment temperature, it comes up to the maximum value at 400 ℃, but it decreases gradually if the temperature rises continuously. The most favourable abrasion resistance was attained after RE-Ni-W-B-B_4C-MoS_2 composite coating being heat treated at 400 ℃. Without heat treating, it is mainly amorphous and partially crystallized, but wholly crystallized after being heat treated at 500 ℃. RE in the composite coating is in the form of CeO_2 and additions of CeO_2 and B_4C can enhance the thermostability of RE-Ni-W-B-B_4C-MoS_2 composite coating.

Key words: electrodeposition; RE-Ni-W-B-B_4C-MoS_2 composite coating; characteristics
CLC number: O 642.11 **Document code:** A

1 INTRODUCTION

By use of the composite electrodepositing technique, codeposition of solid hard particles with metal matrix on the surface to form a composite coating is one of the effective methods to improve the abrasion resistance of material surface[1-6]. Furthermore, the composite electrodepositing technique has many advantages, such as simple process, low cost, operation at ambient temperature and uninfluence on the properties of the inside matrix material, so it holds an important status in the research and development of abrasion-resistant and antifrictional composite materials[7-13]. It is well known that the B_4C particles are abrasion resistant and MoS_2 is self-lubrication materials. The main purpose of this research is to codeposit B_4C and MoS_2 into the coating in order to get abrasion-resistant as well as self-lubricant composite coating.

2 EXPERIMENTAL

2.1 Bath composition and process conditions

The bath composition is as follows: $NiCl_2 \cdot 6H_2O$ 20－30 g/L, complex reagent 60－80 g/L, additive 10－20 g/L, KBH_4 2－3 g/L, $Na_2WO_4 \cdot 2H_2O$ 40－60 g/L, B_4C 40－60 g/L, MoS_2 10－20 g/L, RE 3－5 g/L. The process conditions are J_k 5－10 A/dm^2, t 30 ℃ and pH 13.5.

2.2 Oxidation resistance of composite coating

The oxidization of the coating was run in CHOY type Muffle furnace and the temperature was controlled by KSY-12-16S type instrument within ±5 ℃. In order to measure the high temperature oxidation resistance of RE-Ni-W-B-B_4C-MoS_2 composite coating, the specimens obtained from the optimum bath composition and process conditions were tested at different temperatures for the same holding time or tested for different holding times at the same temperature, respectively. The mass change of specimen after high temperature oxidation can be calculated to determine the oxidation degree of the coating. The mass gain of unit area and unit time of the specimen ($mg \cdot h^{-1} \cdot cm^{-2}$) was taken as the examination index of high temperature oxidation resistance, and the averages of five point values were used.

2.3 Abrasion resistance of composite coating

The coated specimens treated at different temperatures were tested by M-2000 abrasion machine with rotating speed of 400 r/min and loading of 500 N. The mass change($mg \cdot h^{-1} \cdot cm^{-2}$) was taken as the examination index of abrasion resistance. HX-1 microhardness tester was used to measure the hardness

① **Received date:** 2002－11－19; **Accepted date:** 2003－03－03
Correspondence: GUO Zhong-cheng, PhD; Tel: +86-871-5112962; Fax: +86-871-5161161; E-mail: hengdast@public.km.yn.cn

of the composite coatings and the load was 0.98 N.

2.4 Analysis of microstructure and phase structure of composite coating

The microstructure and phase structure of the composite coating were analyzed with ASM-SX scanning electron microscope and Japan 3015 X-ray diffractometer with CuK_α radiation.

2.5 Composition of RE-Ni-W-B-B_4C-MoS_2 composite coating

Boron content in the coating was determined by Auger electron spectrum(AES); RE content was examined by electron spectrometer, and B_4C, MoS_2, Ni and W contents were measured with chemical analytical method, and the average of five point values was used. The composition of the composite coating is 2.5%-3.5% RE, 4.5%-6.5% W, 3.5%-4.5% B, 5.6%-7.8% B_4C, 2.5%-4.5% MoS_2 and Ni.

3 RESULTS AND DISCUSSION

3.1 High temperature oxidation resistance of 3.2% RE-79.2% Ni-5.2% W-3.5% B-5.6% B4C-3.3% MoS_2 composite coating

The mass changes of the coatings at different oxidation temperatures for the same oxidation time(2 h) are shown in Fig. 1. The mass changes of the coatings at the same oxidation temperature (750 ℃) for different holding durations are shown in Fig. 2.

It can be seen from Fig. 1 and Fig. 2 that the oxidation degree of 3.2% RE-79.2% Ni-5.2% W-3.5% B-5.6% B_4C-3.3% MoS_2 composite coating is small when the temperature is lower than 700 ℃, but the mass gain of the coating increases linearly and sharply when the temperature is higher than

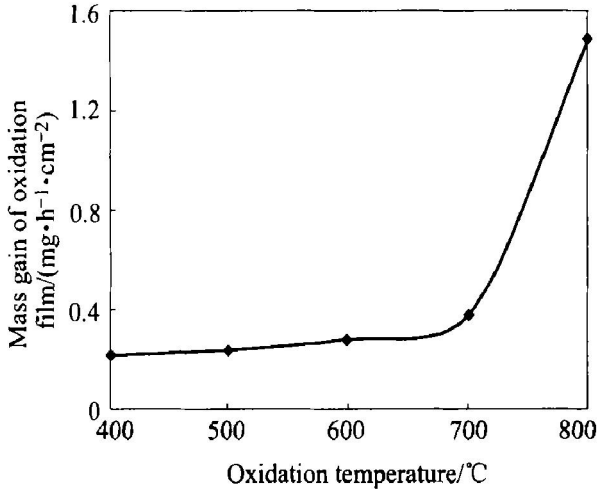

Fig. 1 Relationship between mass gain of coating and oxidation temperature

700 ℃, i.e. the oxidation degree of the coating is large. In addition, at the same oxidation temperature the mass gain of the coating increases with increasing the oxidation time.

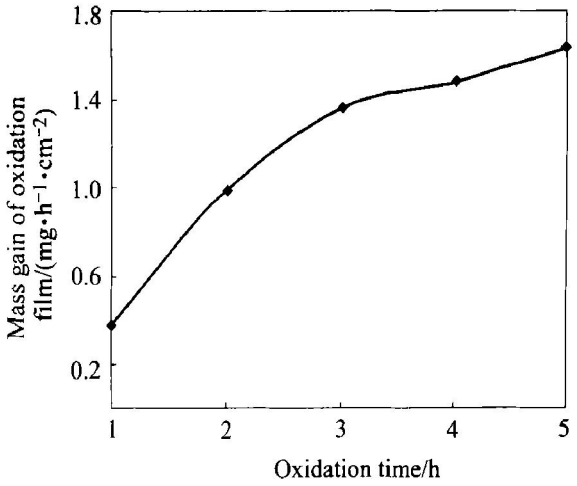

Fig. 2 Relationship between mass gain of coating and oxidation time

3.2 Abrasion resistance of 3.2% RE-79.2% Ni-5.2% W-3.5% B-5.6% B_4C-3.3% MoS_2 composite coating

The effect of heat treatment temperature on the abrasion resistance of the specimen is shown in Fig. 3. It can be seen from Fig. 3 that the abrasion resistance of the specimen after heat treatment is better than that before heat treatment, and the resistance is the best when the specimen is treated at 400 ℃. When the rotating speed is 400 r/min and the load is 500 N, the specimen mass loss is only 0.406 $mg \cdot h^{-1} \cdot cm^{-2}$. Obviously, the composite coating has satisfactory abrasion resistance.

3.3 Hardness of 3.2% RE-Ni-5.2% W-3.5% B-5.6% B_4C-3.3% MoS_2 composite coating

The effect of heat treatment temperature on

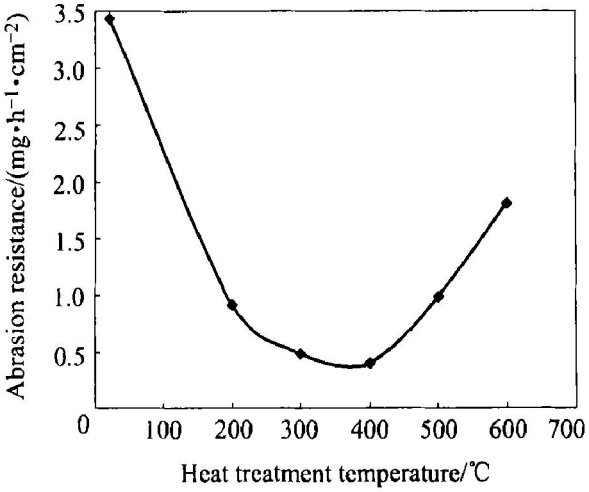

Fig. 3 Relationship between abrasion resistance and heat treatment temperature

the hardness of the composite coating is shown in Fig. 4. It can be seen from Fig. 4 that the hardness of 3.2%RE-79.2%Ni-5.2%W-3.5%B-5.6%B_4C-3.3%MoS_2 composite coating increases with increasing heat treatment temperature, and it comes up to the maximum value(1 368 Hv) when the heat treatment temperature is 400 ℃. If the temperature rises further, the hardness of the composite coating will decrease.

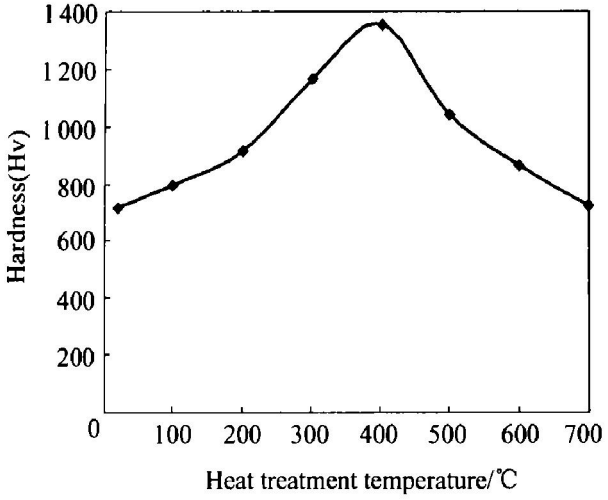

Fig. 4 Effect of heat treatment temperature on hardness of composite coating

3.4 Morphology and phase structure of RE-Ni-W-B-B_4C-MoS_2 composite coating

3.4.1 Morphologies of surface and cross section of composite coating

The effects of electrodeposition conditions on the surface morphology of RE-Ni-W-B-B_4C-MoS_2 composite coatings are shown in Fig. 5.

It can be seen from Fig. 5 that the influence of the elctrodeposition conditions on the surface morphology of RE-Ni-W-B-B_4C-MoS_2 composite coatings are evident. With a rise in current density or bath temperature the grains of the composite coating become coarse and large; on the contrary, the crystal grains are fine and small.

The morphology of cross section of 3.3% RE-79.2% Ni-5.5% W-3.5% B-5.4% B_4C-3.5% MoS_2 composite coating is shown in Fig. 6, and it can be seen that the composite coating contains B_4C and MoS_2 particles, but the distribution of these particles in the coating is uneven, which is mainly due to the worse dispersity of B_4C and MoS_2 particles in the bath.

3.4.2 Phase structure of 3.2% RE-79.2%Ni-5.2%W-3.5%B-5.6% B_4C-3.3% MoS_2 composite coating

The X-ray diffraction patterns of 3.2%RE-

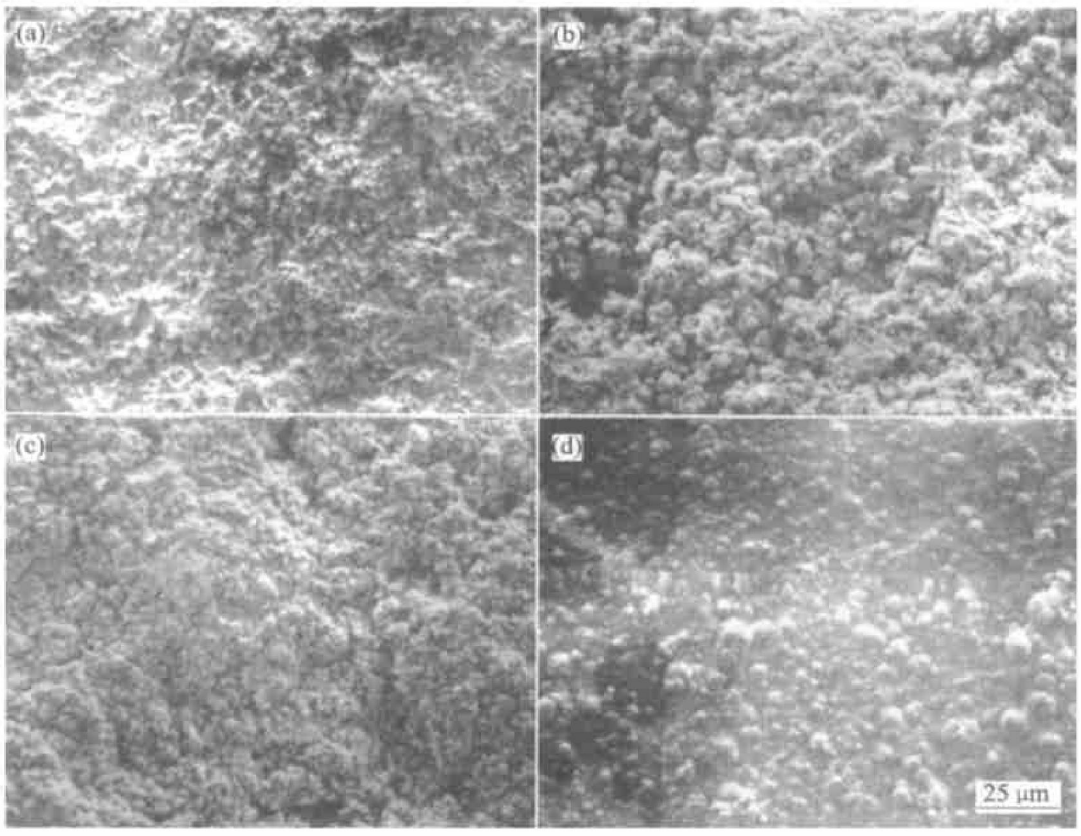

Fig. 5 Surface morphologies of RE-Ni-W-B-B_4C-MoS_2 composite coatings
(a) —J_k= 12 A/dm^2, at 30 ℃; (b) —J_k= 12 A/dm^2, at 60 ℃
(c) —J_k= 10 A/dm^2, at 60 ℃; (d) —J_k= 14 A/dm^2, at 60 ℃

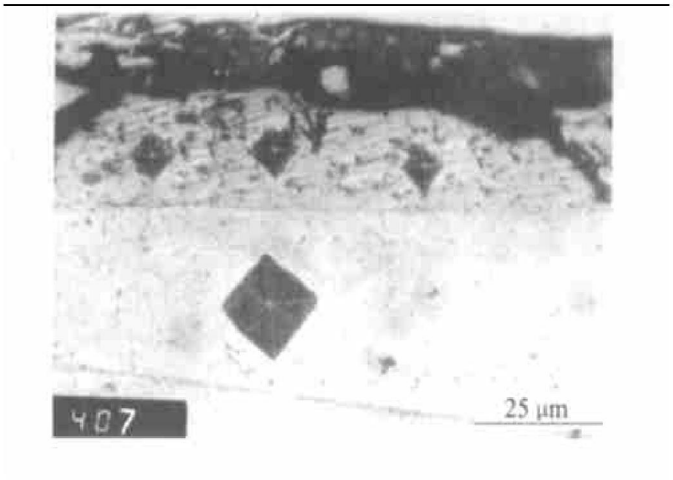

Fig. 6 Cross section morphology of 3.3% RE-79.2% Ni-5.5% W-3.5% B-5.4% B_4C-3.5% MoS_2 composite coating

79.2% Ni-5.2% W-3.5% B-5.6% B_4C-3.3% MoS_2 composite coating are shown in Figs. 7-9. Fig. 7 indicates the phase structure of the electrodeposited composite coating without heat treatment (as-deposited), Fig. 8 shows the phase structure of the coating heat-treated at 500 ℃ for 1 h, and Fig. 9 shows the phase structure of the coating heat-treated at 800 ℃ for 1 h.

Fig. 7 indicates that there appears a relatively unsharp bread peak at $2\theta = 45°$ which is the characteristic peak of amorphous state. The range of the amorphous state is relatively wide, but there are also the characteristic peaks of B_4C, CeO_2(RE) and MoS_2 crystal grains and typical crystalline characteristic peaks of Ni, W, Mo and B, which shows that the as-deposited coating is mainly amorphous and partially crystallized.

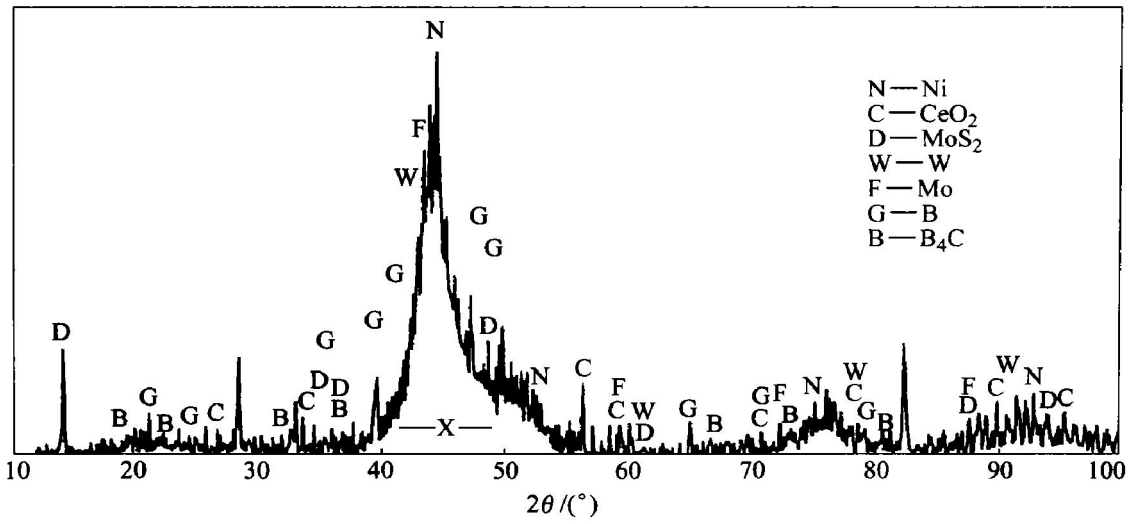

Fig. 7 X-ray diffraction pattern of as-deposited 3.2% RE-79.2% Ni-5.2% W-3.5% B-5.6% B_4C-3.3% MoS_2 composite coating

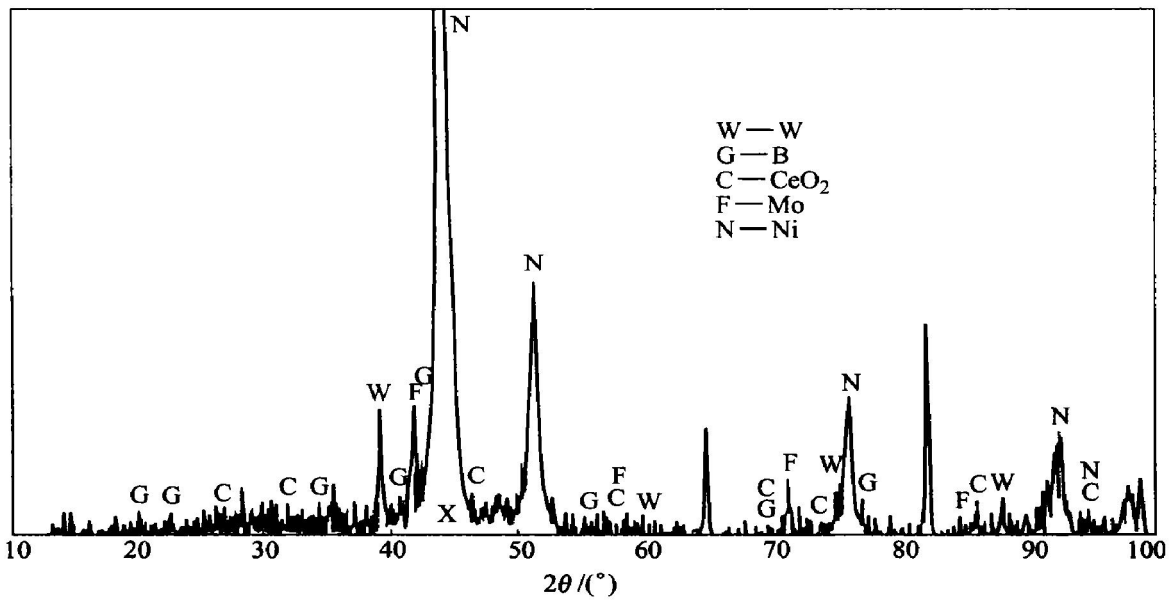

Fig. 8 X-ray diffraction pattern of 3.2% RE-79.2% Ni-5.2% W-3.5% B-5.6% B_4C-3.3% MoS_2 composite coating after heat treated at 500 ℃ for 1 h

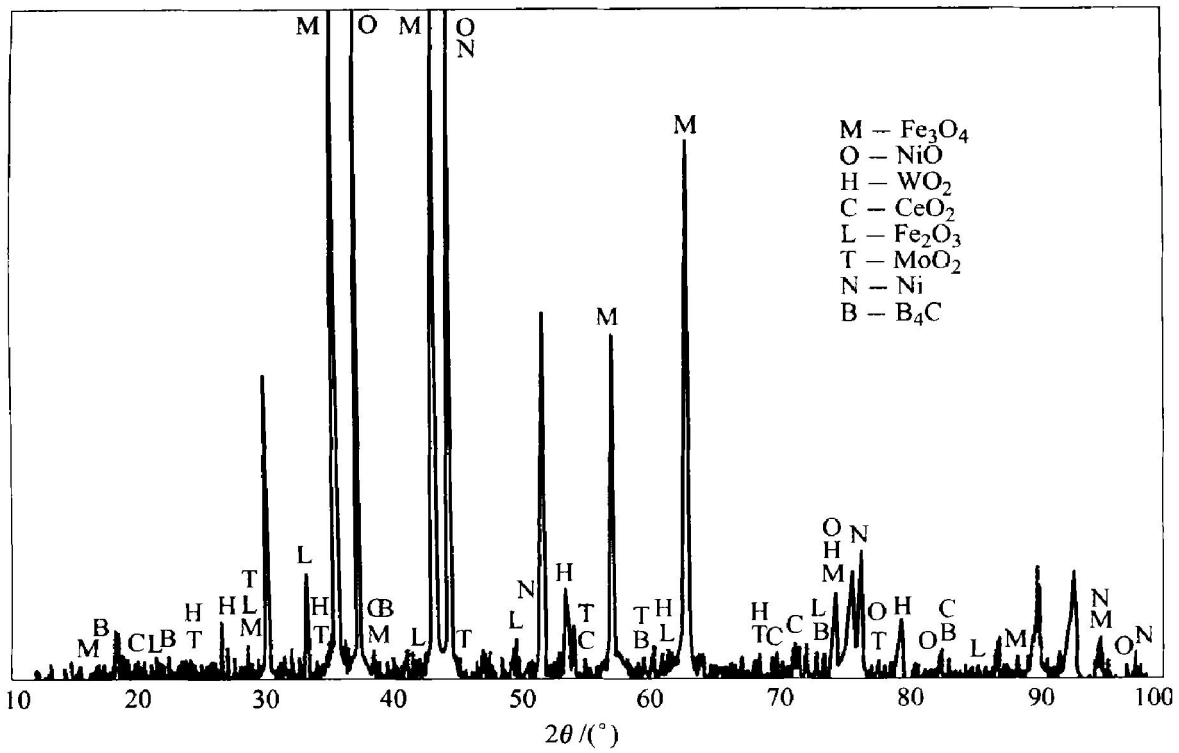

Fig. 9 X-ray diffraction pattern of 3.2% RE-79.2% Ni-5.2% W-3.5% B-5.6% B_4C-3.3% MoS_2 composite coating after heat treated at 800 ℃ for 1 h

In comparison with Fig. 7, the range of the amorphous state in Fig. 8 is obviously reduced and Ni(111), Ni(220) and Ni(222) peaks are more remarkable. In addition, there appear the diffraction peaks of W, Mo, Ni_3B and CeO_2 phases, and these are typical characteristic of crystalline state. This indicates that the crystallization of the composite coating is strengthened after heat treated at 500 ℃ for 1 h.

Fig. 9 shows the X-ray diffraction pattern of 3.2% RE-79.2% Ni-5.2% W-3.5% B-5.6% B_4C-3.3% MoS_2 composite coating after heat treated at 800 ℃ for 1 h. In comparison with Fig. 7 and Fig. 8, the crystalline characteristics of the pattern in Fig. 9 is more obvious—there are few amorphous peak in Fig. 9. At elevated temperature, oxygen in the air diffuses through the composite coating into the matrix, and some of the iron in the matrix is oxidized to form Fe_3O_4 and Fe_2O_3 phases. Ni in the coating is oxidized to NiO, W to WO_2, and MoS_2 to MoO_2. CeO_2 and B_4C are not changed chemically, which indicates that CeO_2 and B_4C are very stable and not decomposed at 800 ℃. This suggests that additions of CeO_2 and B_4C can increase the thermal stability of 3.2% RE-79.2% Ni-5.2% W-3.5% B-5.6% B_4C-3.3% MoS_2 composite coating.

4 CONCLUSIONS

1) As to the high temperature oxidation resistance, the oxidation degree of 3.2% RE-79.2% Ni-5.2% W-3.5% B-5.6% B_4C-3.3% MoS_2 composite coating is small when the temperature is lower than 700 ℃, but the degree of oxidation increases sharply when the temperature is higher than 700 ℃. In addition, the oxidation degree increases with increasing the oxidation time at the same heating temperature.

2) The abrasion resistance of 3.2% RE-Ni-5.2% W-3.5% B-5.6% B_4C-3.3% MoS_2 composite coating is the best after heat treated at 400 ℃.

3) The hardness of 3.2% RE-79.2% Ni-5.2% W-3.5% B-5.6% B_4C-3.3% MoS_2 composite coating increases with increasing heat treatment temperature and it reaches the maximum value(1 368 Hv) at 400 ℃. When the temperature rises continuously, the hardness of coating decreases gradually.

4) The electrodeposition conditions have remarkable influence on the surface morphology of RE-Ni-W-B-B_4C-MoS_2 composite coating. The crystal grains of the composite coating become coarse and large with increasing current density or bath temperature; on the contrary, the crystal grains will be fine and small.

5) The as-deposited 3.2% RE-79.2% Ni-5.2%-W-3.5% B-5.6% B_4C-3.3% MoS_2 composite coating is mainly amorphous and partially crystallized. After heat treated at 500 ℃, the coating is mainly crystallized. After heat treated at 800 ℃, the coating is wholly crystallized. CeO_2 and B_4C are very stable at 800 ℃, which suggests that additions of CeO_2 and B_4C can increase the thermostability of 3.2% RE-79.2% Ni-5.2% W-3.5% B-5.6% B_4C-3.3% MoS_2 com-

posite coating.

REFERENCES

[1] GUO Zhong-cheng, ZHAI Da-cheng, YANG Xian-wan. Microstructure of electrodeposited RE-Ni-W-P-SiC composite coating[J]. Trans Nonferrous Met Soc China, 2000, 10(1): 50-53.

[2] MA Ke-yi, GUO Zhong-cheng, WEN Ming-fen, et al. Combination strengthening process of Ni-W-Ti-SiC composite coating and nitrocarburization[J]. Trans Nonferrous Met Soc China, 1997, 7(4): 148-151.

[3] GUO Zhong-cheng, MA Ke-yi, ZHU Xiao-yun, et al. High temperature oxidation of electrodeposted RE-Ni-W-P-SiC multifunctional composite[A]. Proceeding of the New Century International Conference on Metallurgical High Technology and New Materials of Heavy Nonferrous Metals[C]. Kunming, China, The Nonferrous Metals Society of China, 2002. 466-470.

[4] MA Ke-yi, GUO Zhong-cheng, WEN Ming-fen, et al. Study on structure and properties of Ni-W-SiC composite coating[J]. Acta Metall Sinica, 1997, 10(5): 419-423.

[5] GUO Zhong-cheng, YANG Xian-wan. Effects of rare earth on properties of electrodeposited Ni-W-B-SiC composite coatings[J]. Trans Nonferrous Met Soc China, 2000, 10(3): 538-540.

[6] GUO Zhong-cheng, LIU Hong-kang, WANG Zhi-ying, et al. Properties of electrodeposited amorphous Ni-W-P-SiC composite coatings[J]. Acta Metall Sinica, 1996, 9(1): 44-48.

[7] DENG Lun-hao, GUO Zhong-cheng, YANG Xian-wan. Process conditions of electrodepositing RE-Ni-W-P-SiC-PTFE composite coating[J]. Plating and Finishing, 1999, 18(4): 3-4. (in Chinese)

[8] GUO Zhong-cheng, ZHU Xiao-yun, YANG Xian-wan. Corrosion resistance of electrodeposited RE-Ni-W-P-SiC composite coatings[J]. Trans Nonferrous Met Soc China, 2001, 11(3): 413-416.

[9] ZHU Cheng-yi, GUO Zhong-cheng, LIU Zhong-hua. Structure of Ni-W-P-SiC composite coating reinforced by nitrocarburization[J]. Nonferrous Metals, 1999, 51(1): 65-68. (in Chinese)

[10] GUO Zhong-cheng, DENG Lun-hao, YANG Xian-wan. Abrasion resistacne of electrodeposited RE-Ni-W-P-SiC-PTFE composite material[J]. Materials Protection, 2001, 34(1): 4-7. (in Chinese)

[11] GUO Zhong-cheng, ZHU Xiao-yun, XU Rui-dong, et al. Cathodic process and wear resistance of electrodeposited RE-Ni-W-P-SiC composite coating[J]. Acta Metall Sinica, 2002, 15(4): 369-373.

[12] CHEN Ling, GUO Zhong-cheng, YANG Xian-wan. Structure and characteristics of electrodeposited RE-Ni-W-P-B_4C-PTFE composite coatings[J]. Trans Nonferrous Met Soc China, 2001, 11(6): 887-890.

[13] GUO Zhong-cheng, ZHU Xiao-yun, YANG Xian-wan. Thermodynamics of electrodeposited Ni-B-SiC composite coating[J]. Trans Nonferrous Met Soc China, 2001, 11(5): 800-802.

(Edited by HUANG Jin-song)